Biogeosciences

Open Access

Distribution and biophysical processes of beaded streams in Arctic permafrost landscapes

C. D. Arp[1], M. S. Whitman[2], B. M. Jones[3], G. Grosse[4], B. V. Gaglioti[1,3], and K. C. Heim[5]

[1]Water and Environmental Research Center, University of Alaska Fairbanks, Fairbanks, AK 99775, USA
[2]Arctic Field Office, Bureau of Land Management, Fairbanks, AK 99709, USA
[3]Alaska Science Center, U.S. Geological Survey, Anchorage, AK 99508, USA
[4]Alfred Wegener Institute, Helmholtz Centre for Polar and Marine Research, Potsdam, Germany
[5]School of Fisheries and Ocean Sciences, University of Alaska Fairbanks, Fairbanks, AK 99775, USA

Correspondence to: C. D. Arp (cdarp@alaska.edu)

Abstract. Beaded streams are widespread in permafrost regions and are considered a common thermokarst landform. However, little is known about their distribution, how and under what conditions they form, and how their intriguing morphology translates to ecosystem functions and habitat. Here we report on a circum-Arctic survey of beaded streams and a watershed-scale analysis in northern Alaska using remote sensing and field studies. We mapped over 400 channel networks with beaded morphology throughout the continuous permafrost zone of northern Alaska, Canada, and Russia and found the highest abundance associated with medium to high ground-ice content permafrost in moderately sloping terrain. In one Arctic coastal plain watershed, beaded streams accounted for half of the drainage density, occurring primarily as low-order channels initiating from lakes and drained lake basins. Beaded streams predictably transition to alluvial channels with increasing drainage area and decreasing channel slope, although this transition is modified by local controls on water and sediment delivery. The comparisons of one beaded channel using repeat photography between 1948 and 2013 indicate a relatively stable landform, and ^{14}C dating of basal sediments suggest channel formation may be as early as the Pleistocene–Holocene transition. Contemporary processes, such as deep snow accumulation in riparian zones, effectively insulate channel ice and allows for perennial liquid water below most beaded stream pools. Because of this, mean annual temperatures in pool beds are greater than $2\,^{\circ}\mathrm{C}$, leading to the development of perennial thaw bulbs or taliks underlying these thermokarst features that range from 0.7 to 1.6 m. In the summer, some pools thermally stratify, which reduces permafrost thaw and maintains cold-water habitats. Snowmelt-generated peak flows decrease rapidly by two or more orders of magnitude to summer low flows with slow reach-scale velocity distributions ranging from 0.01 to $0.1\,\mathrm{m\,s^{-1}}$, yet channel runs still move water rapidly between pools. The repeating spatial pattern associated with beaded stream morphology and hydrological dynamics may provide abundant and optimal foraging habitat for fish. Beaded streams may create important ecosystem functions and habitat in many permafrost landscapes and their distribution and dynamics are only beginning to be recognized in Arctic research.

1 Introduction

Channels with regularly spaced deep and elliptical pools connected by narrow runs are a common form of many streams that drain Arctic permafrost foothills and lowlands. These channels are often referred to as "beaded" streams because during summer low flows, pools appear as beads-on-a-string of runs (Oswood et al., 1989). Beaded streams are generally treated in scientific textbooks on permafrost (e.g., Davis, 2001), hydrology (e.g., Woo, 2012), and aquatic ecology (e.g., McKnight et al., 2008), yet to our knowledge field investigations of these systems has been limited to Imnaviat Creek in northern Alaska (e.g., Oswood et al., 1989) and the Yamal Peninsula in Siberia (Tarbeeva and Surkov, 2013).

Table 1. Summary of a circum-Arctic inventory of beaded stream networks in the zone of continuous permafrost based on a survey of high-resolution (< 5 m, summer) imagery available in Google Earth™ during 2012–2013. The relative proportion of high-resolution imagery available in each region was used to estimate the total number of stream networks and drainage density assuming an average network length of 10 km.

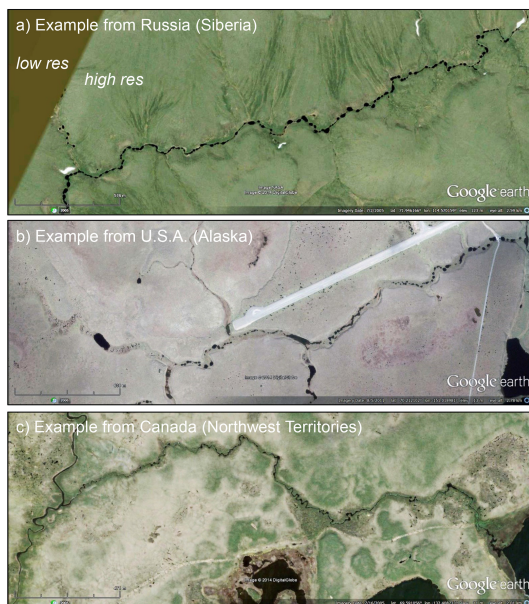| Region	Area (km^2)	Percentage of area with high-resolution imagery (snow-free)	Identified stream networks	Estimated stream networks	Estimated drainage density (km km^{-2})
Northern Canada	2 347 072	9	22	244	0.001
Northern Alaska (USA)	185 907	80	275	344	0.019
Northern Russia	2 123 067	11	148	1346	0.006

Figure 1. Examples of beaded stream networks located by scanning high-resolution (< 5 m) imagery available in Google Earth in **(a)** Russia (Anabar River watershed), **(b)** USA (near Nuiqsut, Alaska), and **(c)** Canada (Tuktoyaktuk Peninsula).

Our understanding of the physical and chemical character of beaded streams mainly comes from Imnavait Creek in the Arctic foothills of Alaska (Oswood et al., 1989). Subsequent studies of this and adjacent systems suggest how beaded morphology functions in permafrost thaw (Brosten et al., 2006), hydrologic storage and hyporheic exchange (Merck et al., 2012; Zarnetske et al., 2007), and thermal regimes (Merck and Neilson, 2012). Thermal stratification in pools up to 2 m deep often occurs in beaded channels during summer low flows (Oswood et al., 1989) and this may play a role in permafrost thaw, hydrologic transport, and nutrient processing as the Arctic climate changes (Zarnetske et al., 2008; Merck and Neilson, 2012). In the winter, foothill streams freeze solid (Best et al., 2005) such that bed sediments thaw slowly and to a limited depth compared to adjacent alluvial channels (Brosten et al., 2006; Zarnetske et

al., 2007). Winter analysis of multiple aquatic habitats on the Arctic coastal plain (ACP), however, shows that beaded streams can maintain liquid water under ice and potentially develop perennially thawed sediments (Jones et al., 2013). These physical regimes of water and energy flow in Arctic streams, coupled with channel morphology and drainage network organization likely also dictate how these ecosystems function as aquatic habitat (Craig and McCart, 1975). Hydrographic analysis of the Fish Creek watershed on the ACP show that beaded streams form the dominant connections between larger river systems and abundant thermokarst lakes, thus influencing both hydrology and the movement of aquatic organisms between habitats (Arp et al., 2012b).

Beaded streams are thought to be a common Arctic thermokarst landform and occur mainly in association with ice-wedge networks of polygonized tundra (Pewé, 1966). The formation of channel drainage in these streams occurs along ice-wedge troughs with mature drainage channels resulting in complete degradation of ice wedges by thermal erosion (Lachenbruch, 1966). Classification of Arctic streams place beaded channels within the tundra class as compared to springs and mountain classes (Craig and McCart, 1975). In foothill watersheds, beaded streams are typically fed by linear hillslope water tracks (McNamara et al., 1999), while on the ACP these channels initiate mainly from thermokarst lakes and drained thermokarst lake basins (DTLBs) (Arp et al., 2012b; Whitman et al., 2011). Based on existing research, it is uncertain whether high densities of beaded streams exist beyond this long-standing focal site (Imnavait Creek/Toolik Lake) and this more recent studied watershed (Fish Creek). Newly published work from Russian permafrost zones is also expanding our knowledge of beaded stream distribution (Tarbeeva and Surkov, 2013). Still, an understanding of their formative processes and the broader watershed functions they provide are currently lacking.

Knowing where beaded streams occur in permafrost landscapes and how these fluvial forms are organized within drainage networks will help advance our understanding of their broader role in watershed, ecosystem, and biological functions across the Arctic. Such analyses will also help in predicting changes in these thermokarst fluvial systems
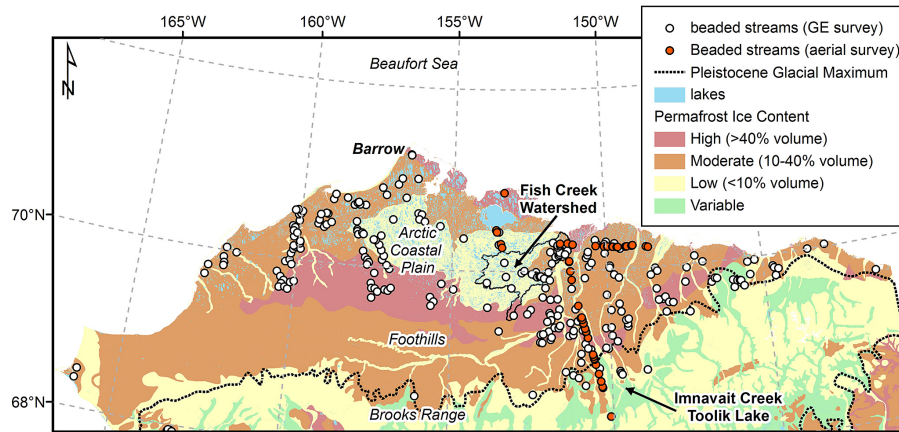
Figure 2. The distribution of beaded streams located using Google Earth and from aerial surveys across the North Slope of Alaska in relation to permafrost ice content (Jorgenson et al., 2008) and the Pleistocene glacial maximum (Manley and Kaufman, 2002). The locations of the Fish Creek watershed (focus area of this study) and Imnavait Creek (focus area of the majority of pervious work on beaded streams) are indicated.
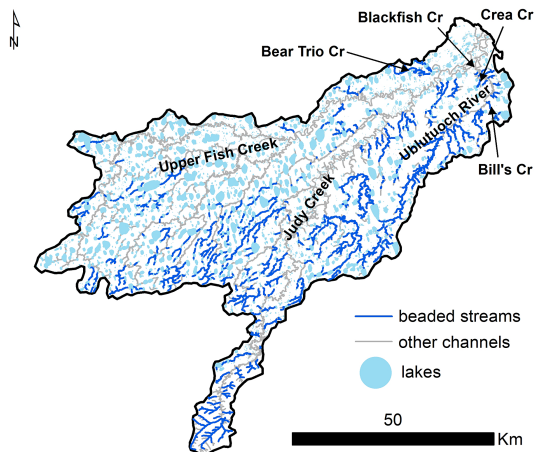

Figure 3. The drainage network of Fish Creek watershed (location shown in Fig. 2) showing all beaded stream networks that were delineated from 2.5 m CIR photography. River systems and individual beaded stream catchments where more detailed field and geospatial studies were conducted for this study are indicated.

with respect to climate and land-use changes and corresponding permafrost responses and hydrologic feedbacks. In this study, we (1) describe the distribution of beaded streams from circum-Arctic to regional scales, (2) explore whether the distribution and variation in beaded morphology helps explain physical functioning, the evolution of beaded streams, and their responsiveness to external drivers, and (3) highlight the important role that these ecosystems serve in aquatic habitat. This work expands our understanding of beaded streams beyond the foothill regions of Arctic Alaska where most of all previous work has been completed, both in terms of fundamental aspects of permafrost and fluvial processes as well as aspects relevant to fish and other aquatic biota.

2   Methods

2.1   Study areas, distribution surveys, and classification

The distribution and abundance of beaded streams were determined by using a nested survey design and a range of survey methods. These nested domains ranged from a (1) circum-Arctic assessment confined to the zone of continuous permafrost using imagery in Google Earth (GE) (Table 1, Fig. 1), (2) aerial transects across landscape gradients on the North Slope of Alaska (Fig. 2), and (3) a census of the Fish Creek watershed (4700 km^2) using high-resolution photography (Fig. 3). We also conducted field studies throughout this watershed and used data from an ongoing monitoring network at several streams in the lower portion of the watershed to characterize biophysical processes and habitat.

The circum-Arctic survey utilized imagery available in GE to identify channels with beaded morphology. This analysis focused on the continuous permafrost zone north of 66° latitude. We utilized the historical image browser function in GE to access the highest resolution imagery (< 5 m) possible for a given region. This analysis focused on portions of Alaska (USA), Siberia (Russia), and northern Canada totaling approximately 4.5 million km^2. We found that most channels with beaded morphology could be identified when scanning images at a 1 : 6000 scale when the imagery had a resolution of 5 m or finer and was mostly snow-free. The availability of high-resolution, snow-free imagery in Alaska was quite good, covering 80 % of the continuous permafrost zone surveyed. In Russia and Canada, the availability of such imagery was much lower, 11 and 9 %, respectively, as of 2013 (Table 1). Prospective beaded channels recognized while scanning were inspected more closely (finer scale) to verify their form and the course was marked as the furthest downstream network point of the continuous beaded channel.
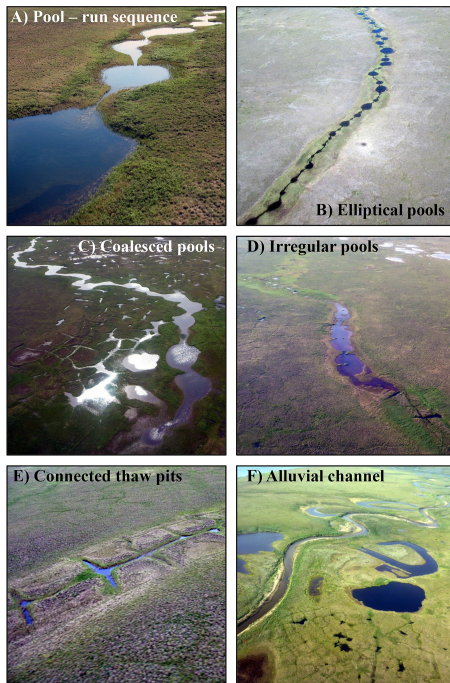
Figure 4. Oblique photographs showing typical pool-run morphology **(a)** and examples of beaded channel forms **(b–e)** compared to alluvial channel **(f)** morphology.

Surface elevation, latitude, and classes of permafrost ground ice were attributed to each point using thematic data sets for pan-Arctic (Brown et al., 1998) and Alaska-focused permafrost and ground ice distribution (Jorgenson et al., 2008) and surface elevation. In order to compare among regions with differing extents of sufficient imagery, we extrapolated the number of surveyed streams based on the proportion of high-resolution imagery available to estimate the total number of beaded stream networks in the circum-Arctic continuous permafrost zone (Table 1). We additionally estimated drainage density of beaded channels based on assuming an average network length of 10 km, which results in only a broad regional average and definitely varies considerably on finer scales.

Regionally (Alaska North Slope) focused aerial surveys in a Cessna 185 were flown on 10 July 2011 on a clear day along three transects. One 270 km transect was from the Brooks Range divide north to the Colville River delta, which moves from glaciated terrain in the upper foothills to vast areas north of the Pleistocene glacial maximum (Fig. 3). Another transect was 130 km from Prudhoe Bay to the lower Fish Creek watershed on the ACP, and a third transect spanned 36 km of land area from Fish Creek to the lands north of Teshekpuk Lake representing an inner to outer ACP gradient. During the transect flights at approximately 150 m elevation, one observer had a sufficient view of approximately 500 m land surface to one side of the plane, thus covering approxi-

mately 220 km^2 of land surface in these surveys. During the flight each stream observed was marked with a GPS, photographed, and later these photographs were inspected to determine which streams could be classified as having beaded morphology.

The watershed census of beaded streams was conducted in the Fish Creek watershed as part of a broader effort to map, classify, and understand watershed hydrography and its role in watershed runoff processes (Arp et al., 2012b). The Fish Creek watershed is located in the northeastern portion of the National Petroleum Reserve – Alaska (NPR-A) on the ACP (Fig. 3). Surface deposits grade from marine-alluvial silt with some pebbly substrates in the east to inactive eolian sand dune fields in the west (Carter, 1981; Carter and Galloway, 2005). The sand-bedded alluvial rivers, Fish Creek (*Uulutuuq*, Iñupiat name) and its tributary Judy Creek (*Iqalliqpiq*), drain this area and form a delta in the Beaufort Sea just west of the Colville River delta. Both rivers begin as beaded streams, Judy in a narrow arm extending into the foothills and Fish in the sand sea. The Ublutuoch River (*Tingmiaqsiuqvik*) also starts as a beaded stream, but maintains this morphology for a longer distance before becoming a gravel-bedded alluvial channel near its confluence with Fish Creek (Fig. 3). All perennial channels in the Fish Creek watershed were delineated from 2002 mid-July color infrared (CIR) photography (2.5 m resolution) in a GIS environment. Streams with beaded morphology were quantified according pool density and size (measured as width perpendicular to the direction of flow) and valley gradient from a 5 m interferometric synthetic aperture radar (IfSAR) digital elevation model (DEM) at a segment scale, typically a 1–3 km length that was representative of individual drainage networks. These segments were also placed into four classes according to predominant pool (channel bead) shape and connectivity to runs: (1) elliptical (round) pools separated by distinct connecting runs (Fig. 4b), (2) coalesced pools (elliptical pools merged together) without distinct connecting runs (Fig. 4c), (3) large irregularly shaped pools often connected by long runs (Fig. 4d), and (4) connected thaw pits in degrading polygonized tundra connected by perennial or ephemeral streams (Fig. 4e). We used this classification to help evaluate if pool form of beaded morphology was correlated with landscape position within the watershed and permafrost ice-content or other thermokarst landforms (e.g., thermokarst lakes and DTLBs). We visited approximately 20 % of these stream channels in the Fish Creek watershed during late July 2011 to verify beaded morphology and classification and to collect additional field measurements, as described below in the next section.

2.2 Geospatial and field measurements

A subset of stream channels mapped and classified in the Fish Creek watershed (Arp et al., 2012b) were used for detailed geomorphic and hydrologic analysis in this study.

Specifically, we targeted a set of each channel class representing beaded streams and alluvial channels (Fig. 4), as well as points of channel initiation. During field visits, we measured stream discharge using the velocity–area method. Along stream reaches equaling 20 or more channel widths (typically 100–300 m), we surveyed the water surface elevation at 5–7 points with an engineer's level, stadia rod, and tape to measure the channel slope. At the same time, channel cross sections that bisected pools were surveyed at 2–3 locations to measure pool geometry as well as the incised zone surrounding the channel (gulch) indicated by riparian vegetation and form.

In order to better understand controls on beaded stream morphology, we conducted similar surveys in the field, and from geospatial data (CIR photography and DEMs) along a longitudinal gradient of Fish Creek and the Ublutuoch River from their headwaters downstream (Fig. 3). For each fluvial system, at least three reaches were studied in the field where the channel had distinctly beaded form and three reaches were studied downstream where the channel had transitioned to an alluvial form. Additional locations were later selected to better refine this transition including identification of sediment sinks (flow-through lakes) or clear-water inputs (lake-fed tributaries) relative to potential sediment sources including contact points with hillslopes and sand dunes, and tributaries originating from DTLBs or upland tundra. Such local controls on delivery of new water and sediment to channels were expected to help explain changes in form downstream, similar in concept to mountain drainage networks flowing through lakes (Arp et al., 2007) and as hypothesized for Arctic drainage networks (Tarbeeva and Surkov, 2013). The total length of channels analyzed for the Fish Creek watershed was about 135 km and the total length of channels analyzed for the Ublutuoch River watershed was about 70 km.

2.3 Analysis of channel change and history

To better understand the evolution of beaded channels we compared the position and morphology of one channel over a 64 a period using high-resolution (1 : 24 000 scale) photography from 1948 (black and white, Naval Arctic Research Laboratory, BW NARL) and 2013 (color-infrared at 25 cm pixel size, Aerometric Inc) located in the Fish Creek watershed. This was done to examine the hypothesis that beaded streams evolve in a manner similar to observed degradation of ice-wedge intersections, but lacking channel connectivity. The 1948 BW NARL photographs were acquired from the University of Alaska Fairbanks GeoData Center and scanned at 1200 dpi. The scanned images were georeferenced with 20 ground control points (primarily, stable ice-wedge intersections) to a light detection and ranging (lidar) data set (detailed below) using a spline transformation and converted to a pixel size of 0.5 m. The 2013 color photography was acquired, by Aerometric Inc., on 4 September to complement airborne lidar data. Manual analysis of both data sets was conducted in

black and white to avoid any bias that may have arisen due to differences in film types and their separation by so many years of time. Particular attention was given to any changes in channel form (location and plan-view dimensions) relative to ambient polygonized tundra within a 100 m buffer of the channel and the presence and dynamics of thaw pits. All stream channels in both images were independently delineated manually and individual pools and ice-wedge intersections with pits marked with a central point. We tracked individual pools (beads) and thaw-pits from 1948 to 2013 and also recorded those features that were observed in one time period but not the other. The channel gulch/riparian corridor was also delineated for both periods, based primarily on the darker (greener) signature of taller sedges, willows, and dwarf birch and moister understory bryophyte communities.

In order to estimate the timing of pool initiation, long-term sedimentation rates, and the depositional environment of pools, we collected sediment cores to analyze sediment stratigraphy and estimate age–depth relationships using ^{14}C dating. In April 2012, two overlapping cores were collected from a large, deep pool in Crea Creek (Fig. 3) to a depth of 75 cm (base of unfrozen talik) using a Russian peat corer. Each core was photographed and subsampled at 5 cm increments with subsamples placed in Whirl-Pak™ bags. Here we identified what appeared to be basal sediments where the channel initiated, as indicated by an organic sediment layer with fibrous terrestrial organic remains sitting above a homogenous and thick sand layer extending down into the base of the talik. We sampled an individual twig from this basal section for ^{14}C dating. Several moss and sedge samples were also collected from above the basal layer in organic-rich, sandy sediments, similar to organic-rich *gyttja* deposited in lakes of the region, for dating as well. Another core was collected from a pool in 2013 at nearby Blackfish Creek (Fig. 3) and macrofossils were collected from above several distinct sand horizons within the core. The plant macrofossils were prepared for analysis with an acid-base treatment and analyzed for ^{14}C content using standard acceleratory mass spectrometry techniques at the NOSAMS (National Ocean Sciences Accelerator Mass Spectrometry) facility at Woods Hole Oceanographic Institute. All radiocarbon dates were calibrated to calendar ages using the IntCal 13 curve (Reimer et al., 2013) and are reported as the mean and 2σ ranges of the calibrated ages.

2.4 Hydrologic monitoring and habitat analysis

As part of an ongoing monitoring program (Fish Creek Watershed Observatory; Whitman et al., 2011), streamflow, water temperature, and other water quality parameters have been recorded at hourly intervals at five stream-lake systems since 2008. These small catchments (Fig. 3) are being monitored by the Bureau of Land Management (BLM) Arctic Field Office to collect baseline data prior to expected changes in land use, primarily new oil development, and associated
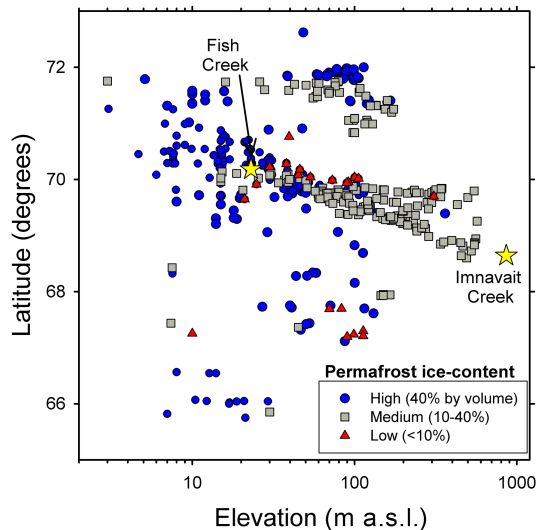
Figure 5. The distribution of beaded stream channels throughout the circum-Arctic in relation to latitude, elevation, and permafrost ground-ice content. Stream networks were identified using imagery in Google Earth in the zone of continuous permafrost where high-resolution imagery was available. The location of streams in the Fish Creek (focus area for this study) and Imnavait Creek (focus area for majority of previous beaded stream research) watersheds are indicated with yellow stars.

Figure 6. Morphological characteristics of beaded streams compared according to pool (bead) density, size, and shape classes (examples shown in Fig. 4 and locations shown in Fig. 3) at the segment scale (1–3 km channel length) in the Fish Creek watershed.

lake-water extraction for ice road construction and facility operations in the NE NPR-A. Stream gauging was conducted using autonomous pressure transducers (Onset U20-001-01) anchored to pool beds, which were corrected to local atmospheric pressure to measure water height. Stream discharge was measured using the velocity–area method with either an ADCP (acoustic doppler current profiler; Flowtracker™) or electromagnetic (Hach™) velocity meter mounted to a top-setting wading rod. Approximately 20 velocity measurements were made per cross section at increments spaced to not exceed 10 % of total discharge. Typically we made 3–4 measurements near the snowmelt peak flow in early to mid-June, 2–3 measurements during peak-flow recession in late June or early July and 2–3 measurements again in late July and late August. Rating curves were fit with a log or power law equation to estimate continuous discharge during the ice-free season; separate high-flow and low-flow rating curves were often required. Based on temperature sensors placed in channel runs and comparison with time-lapse cameras set during several years, we assumed that streamflow ceased during October in most years.

We tested how contrasting beaded stream morphometry and watershed features affected hydrologic residence times and velocity distributions using tracer tests on two stream reaches with contrasting morphology and flow regimes (Fig. 6). At Crea and Blackfish creeks (Fig. 3), we identified 325 and 232 m reaches, respectively, starting and ending at channel runs to ensure initial mixing and sampling of the
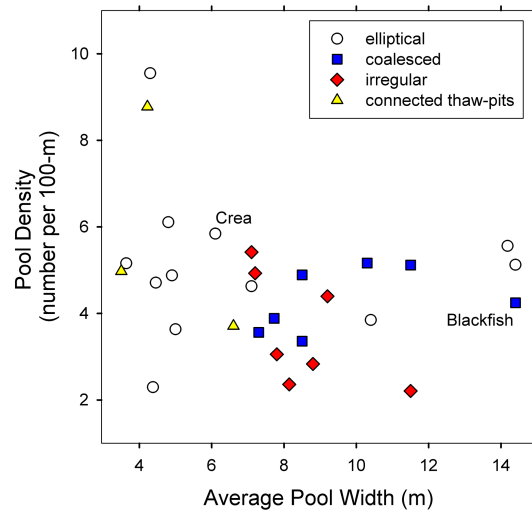
advective flow. Rhodamine WT (RWT), a pink fluorescent dye, was used as a water tracer because it can be detected at low concentrations and only small quantities are required to reach target concentrations, which is an important practical consideration for remote field sites. RWT has low biological reactivity, yet does sorb to organic matter and begins photodegrading after several days of sunlight exposure at low concentrations (Vasudevan et al., 2001). Thus, RWT is not truly conservative,however, is widely used to characterize channel hydraulics and transient storage processes, including previous work in Arctic beaded streams (Zarnetske et al., 2007). Based on targeted downstream peak concentrations of 30 ppb (parts per billion), we made pulse additions of RWT at reach heads and monitored concentration at the reach bottom using a YSI 6600-V2 water quality sonde with a RWT probe. This experiment typically lasted a day or longer to account for all tracer moving through the system. RWT tracer data were then fit with the model One-dimensional Transport model with In-channel Storage and Parameterization (OTIS-P) to estimate advective channel area (A), storage zone area (A_S), dispersion (D), and the storage exchange coefficient (α) (Runkel, 2000). The percentage of RWT recovery averaged 81 % with an average sorption coefficient (λ) of 1×10^{-5} used to account for this loss downstream. A tracer breakthrough curve data was plotted as cumulative solute recovered downstream and converted to velocity distribution by dividing reach length by travel time. RWT injections were conducted at both Crea and Blackfish creeks in mid-June near peak flows, in early July (late peak-flow recession), and late August (low summer baseflow).

Stream thermal regimes were quantified using the same pressure transducers anchored to pool beds that also record

temperature, along with thermistors (Onset U12-015) near the surface of pools (30 cm below) and in channel runs of each beaded stream; all recording at hourly intervals. These paired temperature measurements were used to assess thermal regimes and timing and extent of stratification in pools assuming that a ratio of surface temperature to bed temperature > 1.1 indicated stratification. Using this system, one pool and corresponding channel run have been monitored among five streams year-round from 2009–2013 (Fig. 3). To assess variability in thermal regimes and particularly stratification within stream systems, we selected an additional three pools of varying depth and area in both Crea and Blackfish creeks (Fig. 3) in 2012 and instrumented these with additional bed and surface thermistors. These were retrieved and downloaded in late August 2013.

During the late winters (March and April) of 2010–2013, we visited several of these same beaded stream reaches concurrent with lake-ice, snow, and water chemistry surveys. When opportunities existed, we measured snow depth either with a 3 m avalanche probe or by digging a pit, or both, above frozen pools located with a GPS. Holes were augered through the ice and ice thickness and below-ice water depth was measured using an ice-thickness gauge (Kovacs Enterprises LCC™). We also measured the depth of thawed sediment (talik) using multiple 1.2 m threaded stainless steel rods fitted with a blunt tip and driven with a slide-hammer to the depth of refusal (typically 10–20 pounds with no downward movement). When possible, these late winter surveys were done repeatedly at the same pools including measurements of dissolved oxygen, specific conductance, and pH to assess the quality of overwintering fish habitat.

3   Results and discussion

3.1   Beaded stream distribution

Using available high-resolution imagery in GE across the circum-Arctic, we found 445 individual channel networks located in northern Alaska, Russia, and Canada with beaded morphology (Table 1). This survey was restricted to land areas north of 66° latitude, which was mainly in the zone of continuous permafrost, though two streams identified were within areas classified as discontinuous and three within areas classified as sporadic permafrost. The availability of high-resolution snow-free imagery strongly reduced the number identifiable channels in Siberia and Canada. Extrapolations to the entire region of continuous permafrost based on the area we could accurately survey, suggests greater than 1900 individual beaded stream networks with 13 % in northern Canada, 18 % in Alaska, and 69 % in northern Russia (Table 1). The density of beaded streams in Alaska was estimated to be about 3 times higher than in Russia and 19 times higher than Canada, likely related to its small but wide unglaciated, ice-rich permafrost coastal plain of the Alaska

North Slope relative to abundant mountain and foothills terrain of much of northern Russia and the expansive Laurentian Shield covering much of northern Canada.

In Russia, 148 beaded streams were identified and clustered mainly in several different locations. From east to west these included coastal plains along the Chukchi Sea, lake-rich valley bottoms west of the Kolyma Delta, mountainous headwaters of the Yakutia region, higher elevations of the Yamal Peninsula, and very high densities in the foothills of the Anabar River watershed (Fig. 1a). Recent field studies were completed on beaded streams on the Yamal Peninsula and these researchers also remotely identified channels with beaded morphology in other Russian taiga and steppe terrains using Google Earth (Tarbeeva and Surkov, 2013). Comparatively fewer beaded streams were identified across the Canadian Arctic (22 total) (Table 1). This is likely related to regional geology associated with the dominance of exposed bedrock and thin sediment cover and lack of ice wedges on the Canadian Laurentian Shield. From west to east, small clusters of beaded streams were found on the coastal plain east of Herschel Island and south of the Mackenzie River delta, the lake-rich Tuktoyaktuk Peninsula (Fig. 1c), the coastal plain around the Coronation Gulf and village of Kugluktuk, and the Banks Peninsula within Bathurst Inlet, where high-resolution imagery was available during this GE survey.

Because of greater availability of high-resolution imagery, over 60 % of the beaded streams we located were in Alaska even though this was a much smaller area surveyed (Table 1). The southernmost beaded streams in Alaska were found on the coastal plain of the Seward Peninsula and between Kivalina and Point Hope with an additional cluster higher in the Noatak River valley (Fig. 2). On the North Slope of Alaska, beaded streams were dense and more evenly distributed in the western foothills and along the Chukchi coastal plain. Lower densities of beaded streams were found in the central sand sea region and only a few beaded channels were found on the outer coastal plain of the Barrow Peninsula and north of Teshekpuk Lake. This lack of channels with beaded morphology on the outer coastal plain is perhaps unexpected, given the ubiquitous presence of ice-wedge polygons in which beaded drainage forms. We have observed however that most channels in this region tend to take a plane bed form without alluvial features, which may relate to very high pore-ice content that in addition to wedge-ice makes soils in this region extremely ice-rich, often exceeding 80 % by volume (Brown, 1968, Kanevskiy et al., 2013). The outer coastal plain is also extremely flat with very low drainage densities and very high coverage of thermokarst lakes and DTLBs (Hinkel et al., 2005), such that all fluvial systems are in low abundance and the ones present are strongly lake-affected. On the inner coastal plain and foothills, channels likely develop along moderately sloping terrain with varying densities of ice wedges, but otherwise low pore-ice content. Thus, bead morphology likely develops as ice-wedge

networks thermally erode, yet the expansion of pools and runs is confined to the original ice-wedge casts likely because ice-poor permafrost is more resistant to thermokarst erosion. High densities of beaded streams were also found throughout the Kuparuk River watershed from the foothills to the coastal plain and on the narrower coastal plain east of the Sagavanirtok River to Barter Island (Fig. 2).

Looking at the full set of beaded streams in relation to the ground-ice content of permafrost shows that 50 % were found on high ground-ice content permafrost, 32 % on moderately high ground-ice content permafrost, and 18 % on low ground-ice content permafrost (Fig. 5). Regions with high ground-ice content were typically associated with either epigenetic permafrost along the coastal region and syngenetic yedoma permafrost in the foothills region. Approximately 50 % of all beaded streams were found below 60 m a.s.l. (above sea level) elevation and 90 % were found below 210 m a.s.l. elevation (Fig. 5). Seven beaded streams were discovered above 500 m a.s.l. These were found in both Alaska and Russia. Our survey did not identify the even higher-elevation Imnavait Creek, 861 m elevation (Figs. 2, 5), since the only high-resolution GE imagery for this area was acquired during winter snow cover when beaded morphology could not be observed, demonstrating the limitations associated with this identification approach. However, such snow-covered scenes were relatively rare in most imagery we used. Imnavait Creek, along with 12 beaded streams that were identified in our inventory, occurs above the Pleistocene glacial maximum (Fig. 2) indicating that streams with beaded morphology can readily form in glaciated terrain.

In our aerial surveys across the Alaskan North Slope, we located 43 beaded streams from three transects covering 436 km of flight lines or approximately 220 km^2, suggesting a density of 0.20 streams per square kilometer or a drainage density of roughly 0.10 km km^{-2}. Comparing transect lines to landscape classification of permafrost ground-ice content shows that these surveys covered (29 %) low, (59 %) moderate, and (12 %) high categories (Fig. 2). However, of the recognized beaded streams along these courses, a much higher proportion was associated with moderate ice-rich permafrost (76 %). Only three streams occurred on high ground-ice content permafrost, two on very flat outer coastal plain areas with glaciomarine sediments, and one in yedoma deposits of the foothills (Fig. 2). The majority of stream channels on the outer coastal plain, with very low drainage densities, would be generally classified as plane bed (Montgomery and Buffington, 1997) or F5-6 from Rosgen's classification (Rosgen, 1994), and would have also been termed lacustrine channels (Arp et al., 2012b) because they are nearly all mostly fed by lakes. Still, polygonized tundra tends to be more pronounced and uniform in this region, and so a general lack of channels with beaded morphology was unexpected.

Beaded streams in the Fish Creek watershed range in elevation from 6 to 125 m and the full range of permafrost, ground-ice contents (Jorgenson et al., 2008). We invento-ried 126 beaded streams as individual catchments or drainage networks within this 4700 km^2 watershed located on the inner Arctic coastal plain of northern Alaska (Fig. 3). Based on previous analysis of lakes, streams, and river channels here (Arp et al., 2012b), beaded streams represent 1168 km of channel length or 47 % of the entire fluvial system. The equivalent drainage density of beaded stream channels is 0.25 km km^{-2}. Estimated drainage densities for the broader regions surveyed with GE were far lower compared to this watershed (Table 1).

Since the majority of beaded streams on the ACP initiate as first-order channels below thermokarst lakes or DTLBs (Arp et al., 2012b), their distribution throughout the Fish Creek watershed is linked to lake distribution (Fig. 3). The exception to this pattern is in the headwaters of Judy Creek, which form a narrow arm extending into eolian silt deposits with bedrock outcrops. In this area, lake densities are low and many streams initiate as colluvial channels (Arp et al., 2012b), which then transition to beaded morphology downstream, similar to patterns reported for the higher-elevation foothills of the Kuparuk watershed (McNamara et al., 1999). An example of this drainage pattern is also evident in Fig. 1a. Thirteen percent of all beaded streams in the Fish Creek watershed are located within this region of ice-rich eolian loess. Relatively lower densities of beaded streams occur in the eolian sand sea regions (western half of Fish Creek watershed) where permafrost is classified as having low ground-ice content (Fig. 2) and where most lakes formed between relict dunes (Jorgenson and Shur, 2007) and are up to 20 m deep (Arp et al., 2012b). The highest densities of beaded streams occur in the lower Fish Creek watershed where surface geology is dominated by alluvial and marine silts and sands with some pebbly deposits and permafrost is moderately ice-rich (Carter and Galloway, 2005). Our results suggest some variation in beaded stream distribution within the inner coastal plain, particularly with lower densities associated with eolian and alluvial sand deposits and higher densities on marine and loess silt deposits. However, we still find that beaded streams are often the dominant form of low-order channels throughout a wide range of permafrost terrain on the Alaska North Slope and this is likely the case in much of northern Russia as well (Tarbeeva and Surkov, 2013).

3.2 Morphology in relation to landscape and watershed positions

Since abundant large, deep pools are the defining characteristic of streams with beaded morphology, we initially classified and quantified these channels according to pool (bead) morphology and density (Fig. 6). On a reach scale (hundreds of meters) or segment scale (up to several kilometers between tributary junctions), pool density, form, and size was often distinct. However, on a more extensive drainage network scale, which is the scale we used for classification, pool density varied to a greater extent. Counts of pools from

high-resolution CIR photography showed densities ranging from 2 pools per 100 m of channel up to 10 per 100 m (Fig. 6). Lachenbruch (1966) suggested that polygon spacings range from 5 to 50 m based on variation in ground strength and the width of stress relief zones, which approximately matches the range of beaded densities reported here. This indicates that local controls, such as size, pattern, and form (i.e., low- and high-centered polygons) of tundra or broader-scale thermokarst landforms such as DTLBs (Frohn et al., 2005; Hinkel et al., 2005), may be the main cause of such variability in channel morphology.

Of the 126 individual beaded channel networks in the Fish Creek watershed, 40 % were classified as elliptical with distinct connecting runs, 17 % had mostly coalesced pools and short or non-existent runs, 34 % had predominantly irregularly shaped pools, and the remaining 8 % were classified as connected thaw pits (Figs. 4, 6). The majority of beaded channels are shown to initiate from either lakes and DTLBs (Arp et al., 2012b) and these took a wide range of pool forms downstream. In the Fish Creek watershed, most channels with small elliptical pools were located in the higher elevation areas associated with eolian sand and loess deposits compared to lower elevation marine sand and silt deposits. Whether this pattern relates to size and form of ice-wedge networks that develop in sandy soils or how eroding sandy soils moderate expansion by infilling pools or interactions with vegetation deserves further consideration. The other channel classes were more evenly distributed throughout the watershed and by surficial geology.

Comparing channels of the entire watershed by individual slope and drainage area helps us to understand how the larger drainage network is organized from channel initiation points (channel heads) to larger alluvial sand-bedded channels (Fig. 7). This slope–area relationship is consistent with patterns more universally observed across a wide range of drainage networks (Montgomery and Buffington, 1997; Montgomery and Dietrich, 1989; Whiting and Bradley, 1993). In the Fish Creek watershed, channels initiating from hillslopes are steepest with slopes averaging 2 % and with drainage areas $< 1 \, km^2$. Channels initiating from lakes, which all form beaded streams, had average slopes of 0.4 % and drainage areas $> 1 \, km^2$ (Fig. 7). Channel initiation thresholds reported for the foothill's beaded stream Imnavait Creek are $0.02 \, km^2$ (McNamara et al. 1999) – roughly 1 and 2 orders of magnitude smaller than hillslope- and lake-initiated channels, respectively, in this ACP watershed. Because beaded channels compose approximately half of the drainage network in the Fish Creek watershed (Arp et al., 2012b), they correspondingly have a wide range of drainage areas ($2–54 \, km^2$) and slopes ($< 0.1–0.8$ %) (Fig. 7). Analysis of beaded channels in Yakutia, Russia, show a narrower range of drainage areas ($3–10 \, km^2$) with slopes smaller than 0.2 % (Tarbeeva and Surkov, 2013). Alluvial channels form the higher-order portions of most drainage networks and in

Table 2. Comparison of beaded stream morphology and ambient thermokarst features between black and white photography acquired in 1948 and color infrared photography acquired in 2013 for a 2.7 km segment of Crea Creek in the lower Fish Creek watershed.

Attribute compared	1948	2013
Pools		
number	132	134
total area (m^2)	7861	8334
mean area (m^2)	59.6	62.2
number unique	23	25
Gulch/riparian zone		
total area (m^2)	221 802	241 247
mean width (m)	82.1	89.4
Thaw pits		
total number	74	66
number unique	55	47

the Fish Creek watershed they typically begin at drainage areas $> 40 \, km^2$ and channel slopes smaller than 0.03 % (Fig. 7).

To better understand how beaded streams fit within fluvial systems of the ACP and evaluate what controls their morphology, we selected two drainage networks for more detailed analysis of longitudinal channel dynamics from headwaters downstream (Fig. 8). Fish Creek has its headwaters near the western divide of the watershed at 78 m a.s.l. It is located entirely within the eolian sand sheet and initiates from a deep depression lake (Fig. 3). This channel network first flows through several more depression lakes and in between maintains a classic beaded morphology (Fig. 4a). Over the next several kilometers, the channel cuts through both vegetated and unvegetated sand dunes, which likely supply coarse sediment. The channel also contacts steeper hillslopes that could contribute sediment as well. This portion of the channel appears transitional since reaches of beaded morphology are interspersed with more sinuous channels having point bars and meander cut banks (Fig. 8a). At kilometer 20 downstream, the channel steepens considerably below a tributary fed by a DTLB and then cuts through two more sand dunes, before taking a more even slope for the remaining 110 km with sand-bedded alluvial characteristics. Thus, Fish Creek quickly transitions from beaded to alluvial morphology likely because of ample sediment supply associated with the eolian sand landscape (Fig. 6a).

The other system we analyzed, the Ublutuoch River (Fig. 3), begins at a lower elevation than Fish Creek, 58 m a.s.l., in the southern portion of the watershed at the eastern margin of the eolian sand sheet. The channel initiates from a large set of coalesced depression lakes, totaling about 5 km^2, seen as the flat profile in Fig. 8b. The first 12 km of this stream are relatively steep with a regular density of pools typical of beaded morphology. Several oxbow lakes occur lower in this segment, indicative of channel migration, but the
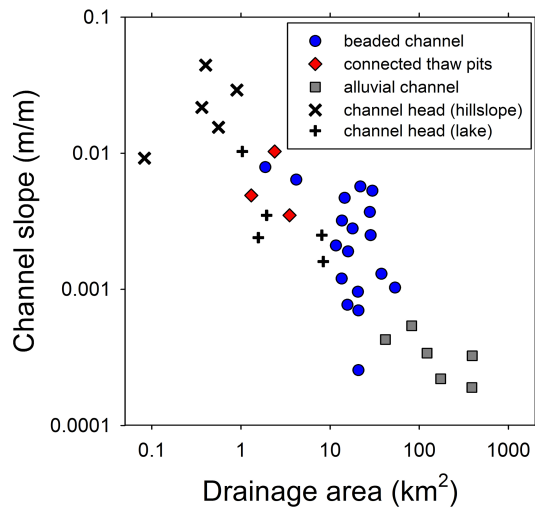
Figure 7. The organization of the major channel forms and channel initiation points (heads) in the Fish Creek watershed are shown in relation to drainage area and channel slope (measured from a 5 m DEM).

Figure 8. Headwater to downstream patterns of a beaded stream originating in the eolian sand deposits, Fish Creek **(a)**, compared with a beaded stream originating in alluvial–marine deposits, Ublutuoch River **(b)**, showing changes in channel elevation and the density of pools and oxbow (meander-cutoff) lakes relative to sediment sources and sinks.

Ublutuoch then flows through several more lakes, likely trapping all sediment and resetting the system to a beaded form with a flatter slope. At kilometer 24 downstream, a tributary from a large DTLB enters from the north and, at this point, the channel starts taking a more sinuous form with oxbow lakes and other floodplain features (Fig. 8b). We suggest that this segment of stream from kilometer 24 to 56 is transitional between beaded and alluvial morphology – a much longer transition than was observed along the upper Fish Creek. Surrounding uplands here are entirely within the zone of marine silt and sand without distinct sediment contributions from adjacent sand dunes. Near the end of the segment, the channel becomes much more sinuous with oxbows and meander scars becoming evident, yet regular pools (beads) persist. At kilometer 56, the stream contacts a distinctly higher hillslope that we think supplies sediment to the channel and after which it takes on a distinct alluvial form lacking any evenly spaced beaded morphology (Fig. 8b). During the entire transitional channel course, the slope is nearly constant at about 0.02–0.04 %. It then flattens greatly to < 0.01 % over the last 5 km and becomes quite deep (exceeding 5 m in some pools) and very sinuous (2.3) with high, regular banks before its confluence with Fish Creek.

3.3 Channel change and formation

To evaluate the hypothesis that beaded streams form in ice-wedge networks and that pools progressively expand over time, more detailed studies were conducted in one system, Crea Creek, in the lower Fish Creek watershed (Fig. 3), to look at decadal-scale changes and estimate its time of formation. Using remote sensing change detection over 64 a, we found no changes in the channel position along this 2.7 km
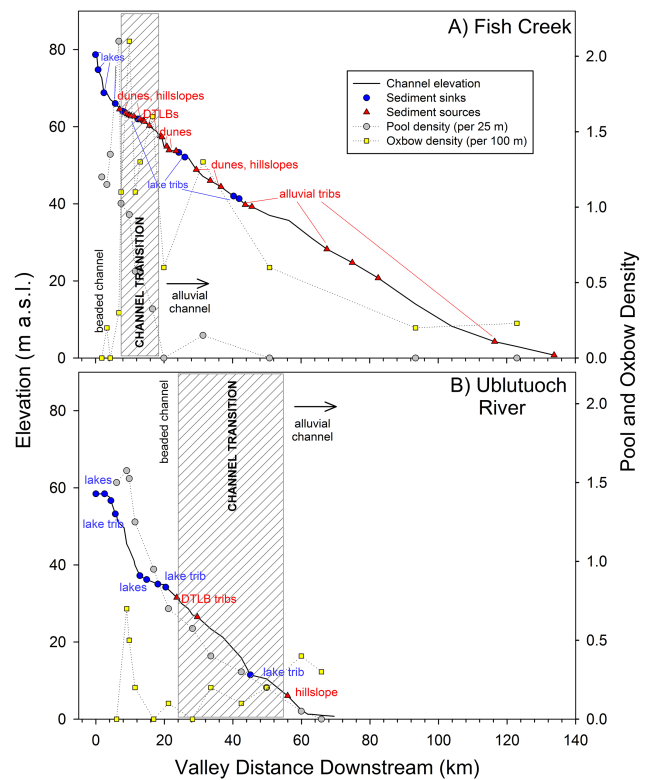
segment (Fig. 9). The total number of pools in this segment remained relatively stable, though tracking individual beads showed that 18 % disappeared or could not be observed from 1948 to 2013 and a similar number of new pools (19 %) were identified in 2013 that could not be observed in the 1948 imagery (Table 2). The majority of these were very small (diameters < 4 m) and we think it is likely that changes in vegetation or variation in water levels between images may have obscured their detection. The mean pool size in 1948 was 60 m^2 compared to 62 m^2 in 2013, resulting in little net change in total pool area over this period. Tracking the size of individual pools found in both images showed that about one-third shrank by more than 10 % surface area, about one-third expanded by more than 20 % surface area, and the remaining pools were essentially unchanged. Thus, our analysis suggests progressive expansion of these thermokarst landforms, yet the channel course appeared entirely unchanged over this period. In comparison to other thermokarst landforms, thermokarst lakes in this region also progressively expand their lake basins, 0.10 m a^{-1} on average (Jorgenson and Shur, 2007), but can drain catastrophically if a shoreline expands beyond a lower gradient or is breached by another lake
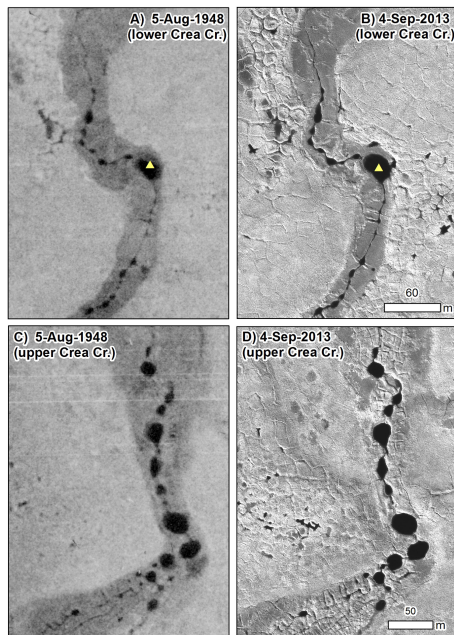
Figure 9. Comparison of two segments of the Crea Creek channel in 1948 **(a, c)** and 2013 **(b, d)** showing that pools, the riparian gulch, and adjacent thaw pits can be clearly observed in each image. The location of a sediment core collected for ^{14}C dating is indicated with a yellow triangle (location of Crea Creek is shown in Fig. 3).

or migrating river (Grosse et al., 2013). Alluvial channels on the ACP are considered highly dynamic and often with very high rates of bank erosion due to interactions with permafrost such that major changes in channel course can occur over short time periods (Scott, 1978). Our observations of a stable course along Crea Creek over 64 a, along with an apparent lack of beaded channels that appear abandoned on the ACP, suggest long-term behavior more similar to bedrock channels (Wohl, 2000). However, Tarbeeva and Surkov (2013) suggest the beaded streams are transient features and become easily filled with sediment from headwater thermokarst and other hillslope erosive processes. We suggest that sediment delivery plays a role in how beaded streams transition to other fluvial forms, but his typically operates at lower positions in the watershed.

We also delineated the riparian zone or gulch of this beaded stream, indicated in plan view by higher moisture and the contrast between upland tussock tundra and vegetation composed of willows, tall sedges, and dwarf birch, to see if other changes beyond the main channels were evident (Table 2). Such changes could correspond to progressive subsidence of ice-rich permafrost by thermokarst degradation or shrub expansion as has been noted throughout many areas of the Arctic (Sturm et al., 2001). Consistent with what can be observed in the shorter reaches in Fig. 9, the overall change in riparian gulch width was slight, a 9 % increase (Table 2). Analysis of repeat photography in this same area

has shown a recent increase in degrading ice-wedge polygons to form thaw pits (Jorgenson et al., 2006). We also recorded and tracked thaw pits (ice-wedge junctions with ponded water) between the two images within a 100 m zone on either side of the channel, but outside of the riparian gulch. This showed a somewhat similar pattern as that found when tracking pools in the channel of Crea Creek. In total, we found 120 individual thaw pits or 1 pit per 2500 m^2, typically in clusters associated with high-centered polygons. In 1948 we found 74 thaw pits, 55 of which were not observed in 2013, and in 2013 we found 66 thaw pits, 47 of which were not observed in 1948 (Table 2). This suggests that thaw pits may progress through a form of succession in which they degrade, collect water, paludify and/or partly drain or dry, such that detection is obscured after several decades. This is a similar sequence to that demonstrated for denser networks of thaw pits in polygonized tundra in adjacent upland areas of the Fish Creek watershed (Jorgenson et al., 2006). We suggest that beaded channels may evolve in a similar manner with most pools gradually expanding and some contracting with changing vegetation. Such behavior seems particularly apparent in viewing coalesced beads of some channels (Fig. 4c). Yet our impression based on this photographic comparison and qualitative observation of other channels with repeat photography is that channel courses and networks appear to behave more like bedrock channels that are set in place and potentially very old.

Analyzing the stratigraphy and geochronology of sediments in a large pool of Crea Creek may attest to the timing of stream channel formation and the depositional environment since initiation. A fibrous, organic-rich layer with abundant terrestrial plant material separated the transition from organic-poor, medium-grained sand to organic-rich, silty sediment that is the uppermost unit – we interpreted this layer as basal sediments that were dated to 9.0 (±40), and 13.6 (±215) ka cal BP (before present) (Fig. 10). The terrestrial macrofossils (shrub twigs) in this fibrous unit and the two dates that span 4 ka suggest this layer may have been a terrestrial soil that persisted for millennia on top of eolian or alluvial sand deposits, but predated the initiation of the beaded stream pool. Alternatively, this layer may represent the depositional environment of an early stage of the beaded stream pool where terrestrial vegetation was overhanging and being deposited, and adjacent soils were being eroded by ice-wedge degradation and supplying a range of reworked material with different ^{14}C ages to be deposited onto this fibrous layer. Regardless, we interpret the 9.0 ka moss macrofossil sampled from the upper portion of the fibrous layer to be a conservative upper limit age on the initiation of the beaded stream pool. At this time, we do not know whether the lower limit of this age estimate is near the 9.0 ka time period, or represents the late Holocene. The large age gap from 9.0 ka at 42 cm to ∼ 0.7 ka at 22 cm suggests that either a water-level lowering event caused a hiatus of sedimentation through much of the Holocene, or that high-flow events
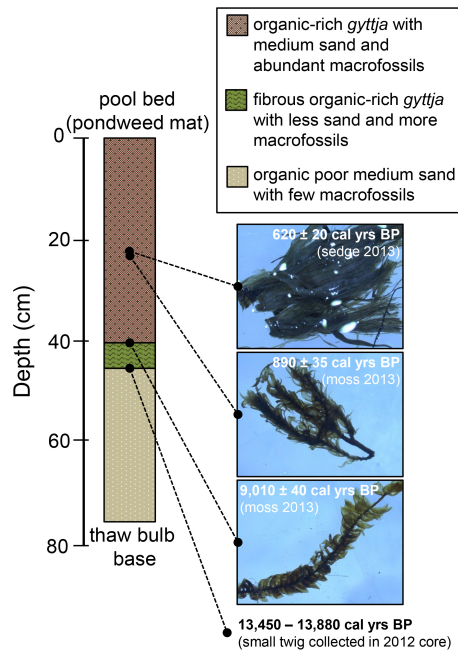
Figure 10. Diagram of generalized sediment core stratigraphy from a large pool in Crea Creek (indicated in Fig. 9) collected in both 2012 and 2013 showing the location of macrofossil fragments collected for radiocarbon dating. The sharp transition from organic-rich *gyttja* to medium sand is interpreted to be the base of the pool at its time of formation.

Figure 11. Late winter profiles (March or April) of several pools (beads) surveyed in multiple beaded streams from 2010 to 2013 ("?" indicated that no measurement of thawed sediment depth was attempted). An example photograph from one pool surveyed in 2013 shows a 1.9 m tall person (G. Grosse) standing on the frozen pool surface for scale.

or other processes eroded the sediment deposits representing most of the Holocene (Fig. 10). However, there was no preserved wetland or terrestrial soil layer interrupting the *gyttja* unit, which would have accompanied a water-lowering event. The Crea beaded stream pool we examined appears to have had episodic sedimentation during the Holocene that is periodically eroded by either high-flow events or ice scouring.

The stratigraphy and ^{14}C dates from a core in a deep pool in Blackfish Creek also suggest unconformities in sedimentation of beaded stream pools. The Blackfish pool had sandy organic-rich *gyttja* with several 3–6 cm bands of coarse sand that graded upward to fine sand. These suggested upstream scouring events that mobilized and transported high- and coarse-sediment loads episodically, potentially from the catastrophic drainage of upstream lakes. A number of DTLBs occur upstream of this site and their drainage dates are currently unknown, but may correspond to these events. The basal age of this unit from a sedge fragment yielded a date of 590 (±30) a BP, considerably younger than we found at Crea Creek (Fig. 10). A paired sedge and willow macrofossil extracted from above a coarse sand horizon at 20–30 cm indicated ages of 1430 (±25) a BP and 125 (±25) a BP. Our interpretation of this core and analyzed ages is that the basal material was either not reached or had been remobilized and that a number of very high-flow events in this stream's recent history had deposited upstream material of varying ages.
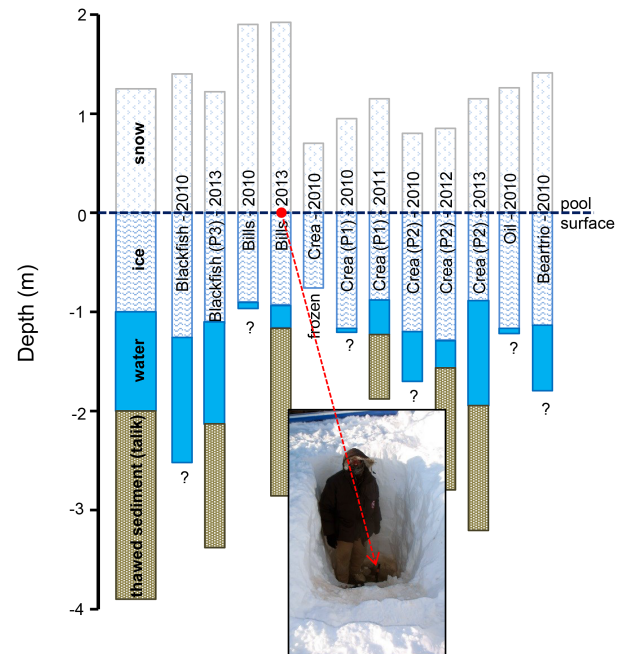
These flow events may have partially eroded some of the late-Holocene record and/or deposited reworked macrofossils, which yielded less certain ^{14}C ages. The depositional environments of beaded streams seem discontinuous and difficult to interpret because of unconformities and reworked plant macrofossils. In the right situation, however, pool sediments may record upstream watershed events such as lake drainage, as we think is preserved in the Blackfish Creek core. At this time, the typical lifespan of the beaded streams we studied remains uncertain, but our best estimate places the Crea Creek channel's formation near the Pleistocene–Holocene transition. The Blackfish Creek core was much more complicated and provided no apparent clues to the age of this beaded channel.

3.4 Physical processes affecting morphology and habitat

3.4.1 Winter processes

Because winter is the dominant season in the Arctic and most beaded streams are ice-covered and likely stop flowing from October to late May or early June, understanding their state during this period is of great interest. An important characteristic of beaded stream channels on the ACP is that their often deep gulches, 0.5–2.0 m, rapidly fill with blowing snow early

in the winter, effectively leveling the snow-surface topography with the surrounding tundra. This deep snow insulates ice on pool surfaces, reducing its rate of thickening, and impacting soil active-layer dynamics as well. Measured snow depths above beaded streams averaged 122 cm and ranged from 70 cm on a small pool in Crea Creek to 192 cm above a pool in Bill's Creek (both in the lower Fish Creek watershed) (Fig. 11). In contrast, surrounding tundra snowpack rarely exceeds 40 cm depth by late winter. Not only does this thick snowpack insulate ice and soil, but it also persists much longer in the spring and contributes a much larger portion of snow-water per unit area directly to runoff (Arp et al., 2010). From 12 beads we surveyed from 2010 to 2013, only one was found to be entirely frozen to the bed by March or April (Fig. 11). A more detailed and extensive survey of water below ice was conducted in March and April of 2013 using ground-penetrating radar (GPR) and high-resolution synthetic aperture radar (TerraSAR-X) in this area and found the majority of pools had liquid water below ice (Jones et al., 2013). The average ice thickness of pools surveyed was 106 cm and ranged from 89 to 129 cm (Fig. 9). For comparison, lake ice thickness in this same region and years ranged from 118 cm in 2011 to 171 cm in 2013 (Arp et al., 2012a; Jones et al., 2013). The average depth of water we found below the ice was 44 cm and ranged from 4 up to 106 cm (Fig. 11). This water was typically under pressure from ice expansion and the weight of snow, such that upon drilling through the ice, water typically floods the frozen pool surface. On at least two occasions live fish (Alaska blackfish, *Dallia pectoralis*) were pushed out of the drill hole to the surface by flowing water during these surveys. Monitored dissolved oxygen levels in one bead showed a rapid drop to hypoxic conditions by mid-January and measurements in March typically showed levels below 5 % of saturation or $< 1 \, \text{mg L}^{-1}$. Alaska blackfish, however, are known to tolerate such conditions (Scott and Crossman, 1973; Crawford, 1974), providing evidence that some beaded stream pools can function as overwintering habitat for select Arctic fish species. While we suspect that these stream pools are not preferred overwintering locations for most fishes, these relatively warm unfrozen sediments may be important habitat for invertebrate and microbial communities.

Despite the relatively small diameter of pools, thawed sediment underlie most of them and measured depths averaged 120 cm and were up to 170 cm in one pool with sand-gravel sediment (Fig. 11). Similar talik depths are reported for pools or broadenings in beaded channels in Russia (Tarbeeva and Surkov, 2013). This suggests that beaded stream channels further disrupt the ground thermal regimes of otherwise continuous permafrost landscapes at a scale relative to their size, whereas large river channels and lakes with floating ice result in taliks reaching tens of meters or more in depth (Brewer, 1958; Lachenbruch et al., 1962). Since 2009, we have been monitoring bed temperatures in a set of pools within beaded stream systems in the lower Fish Creek watershed. Typically winter bed temperatures rapidly approach the zero-degree curtain and average winter temperatures (November–April) consistently average 0 °C (± 0.1). Similarly, mean annual bed temperatures (MABTs) fall within a narrow range averaging 2.9 °C and varying interannually almost entirely according to summer temperatures (Fig. 12a). Such MABTs above freezing also suggest the presence of a talik (Burn, 2002; Ensom et al., 2012), as we confirmed with field measurements. The presence of year-round unfrozen sediment and some liquid water in pools may be an essential factor supporting microbial- and invertebrate-based food webs, which then feed summer productivity and the use of beaded streams as important foraging habitat. Additionally, perennially thawed sediment also likely enhances the survival and productivity of macrophytes that provide additional habitat and forage.

3.4.2 Summer processes

Much of the variation in the MABT of pools is determined by whether pools become thermally stratified during the summer. Monitoring of surface temperatures relative to the pool beds and temperature in the channel runs suggests a wide range of mixing behaviors and stratification regimes among pools both between different stream systems and from pool to pool in a single stream. For example in three beaded streams monitored from 2009 to 2012, a 1.3 m pool never became stratified, another 1.4 m pool was stratified by 10 % or more (i.e., surface temperature / bed temperature > 1.1) for 13 days per summer on average, and a 2.1 m pool had a stratification ratio of 1.2 and was stratified for over a month on average per year (Fig. 12b). This generally suggests that deeper pools stratify to a greater degree and for longer periods. To assess interpool variability, we instrumented an additional three pools in Crea and Blackfish creeks from June 2013 through August 2013 with surface and bed thermistors. In Crea Creek with pools depths of 1.6, 1.7, and 2.0 m, the corresponding average stratification ratios (and durations with ratios > 1.1) were 1.05 (5 days duration), 1.09 (23 days), and 1.03 (4 days), respectively (Fig. 12b). In Blackfish Creek with deeper and coalesced pools, instrumented pools had 1.5, 2.2, and 2.6 m depths and the corresponding stratification ratios and durations were 1.04 (5 days), 1.16 (24 days), and 1.10 (19 days). Thus, there is, as expected, some relationship between pool depth and stratification, but this is generally weak and suggests other factors control how water mixes among different pools. A single densely instrumented pool in Imnavait Creek was shown to stratify in a complex and dynamic manner (Merck and Neilson, 2012), similar to more extensive work completed there originally (Oswood et al., 1989). The velocity of upstream runs and morphology of pools at run inflows is certainly one factor. A steeper run upstream of Bill's Creek was likely the cause of continuous mixing during all flows, ambient air temperatures, and wind regimes, which produced higher MABTs (Fig. 12a) and possibly the deepest talik we measured (Fig. 11).
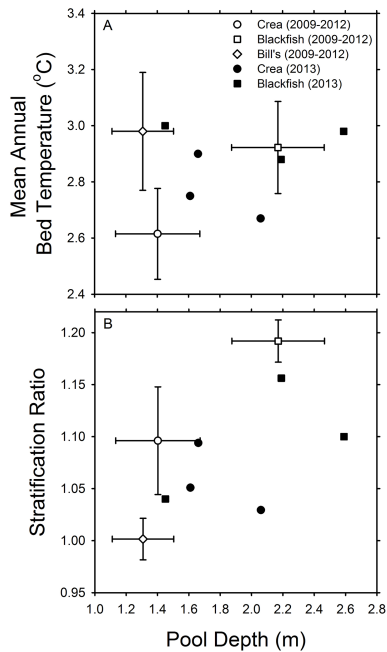
Figure 12. Thermal regime characteristics of single pools at three beaded streams averaged over 4 a (error bars are standard deviations). In 2013, three additional pools within two of these beaded streams were monitored to assess within-stream variability of thermal characteristics. Thermal regimes were characterized by mean annual temperatures at pool beds (**a**) and stratification ratios as the average ratio between the pool surface and bed during the period from July to mid-August in each year (**b**). Pool depths are averaged during the same period that temperature was summarized in each plot.

Figure 13. Streamflow hydrographs and temperature regimes for two beaded streams (Crea (**a**) and Blackfish (**b**) creeks) with contrasting channel and watershed morphology. Bed and surface temperatures were monitored in multiple pools within each reach to document the timing, magnitude, and variation in stratification in relation to streamflow (streamflow is indicated by Q_W, temperatures are indicated at pool beds by T_{bed} and pool surface by T_{sur}, and timing of water tracer injection studies are indicated with red circles by RWT_{inj}; all data are presented as mean daily values from hourly measurements).

The extent and structure of emergent aquatic macrophytes in pools likely also plays a role, where some shallow beads have very dense macrophyte beds (*Potamogeton* spp., *Arctophila fulva*, and *Hippuris vulgaris* are the most common plants) that likely create a rough and thick boundary layer enhancing stratification. Adjacent pools of seemingly similar depth and surface area are often devoid of vegetation, creating greater habitat heterogeneity within beaded stream systems. Variation in water color due to dissolved organic carbon may play some role; however, rarely do beaded streams in this part of the ACP have highly stained water from organic acids as has been observed in other beaded stream systems at foothill locations (Merck and Neilson, 2012; Oswood et al., 1989).

Ecologically, the important point in terms of fish habitat is that within a single beaded stream, varying degrees of mixing and thermal stratification from pool to pool likely create a range of temperature zones that can be utilized to either avoid thermal stress or optimize energetics for foraging and other activities. For example, some salmonids behaviorally thermoregulate by moving to warmer areas after foraging bouts in cooler water in order to accelerate metabolism and as-
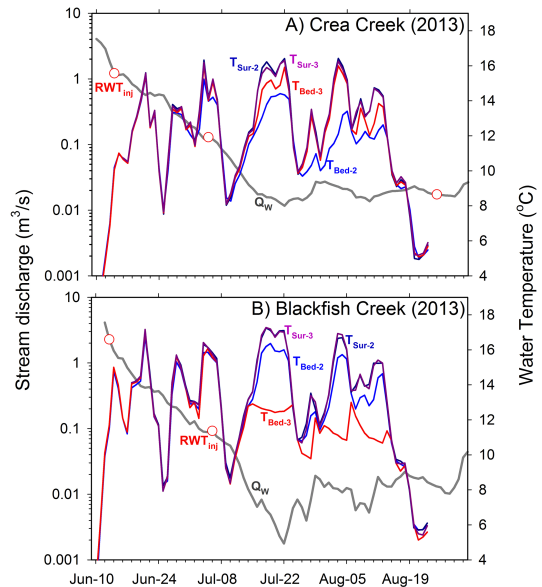
similate more quickly (Armstrong et al., 2013). Stratification within a single bead and heterogeneity in thermal characteristics of nearby beads within a network may provide similar opportunities to behaviorally optimize growth and foraging efficiency during summer. This thermal variability may also play a key role in the distribution of fish prey items, including the forage fish ninespine stickleback (*Pungitius pungitius*) as well as invertebrate and plankton communities (McFarland, 2012).

Similar to the development of stratification in Arctic lakes, stream pools tend to stratify starting in early July following snowmelt runoff and associated cold temperatures and turbulent mixing. An episode of intense summer warming leading to stratification was clearly observed in pools at Crea and Blackfish creeks starting on 9 July 2013 when the surface water temperature rose rapidly from 8 to 16 °C over several days while beds warmed more slowly, albeit to differing degrees (Fig. 13). In Crea Creek, the mean daily temperature difference between the pool surface and bed was as high as 2.5 °C in one pool and only 0.9 °C in the other (Fig. 13a). For the same warming event in Blackfish Creek, levels of stratification were 1.1 °C in one pool and 4.7 °C in the other (Fig. 13b). Another warming event in late July caused even higher stratification, up to 5 °C, in pools of both streams.
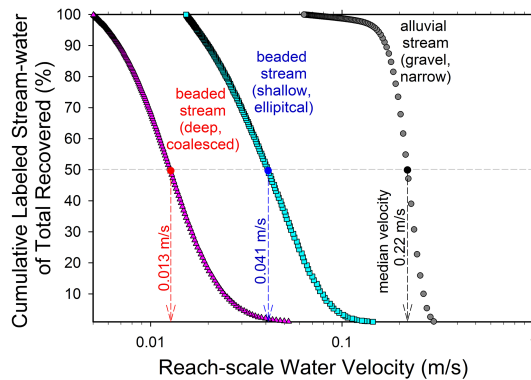
Figure 14. Examples of reach-scale water velocity distributions (reach length/travel time) measured using hydrologic tracer tests (rhodamine WT pulse additions) shown as cumulative tracer recovered downstream. Results from two beaded streams, Crea Creek (blue squares) and Blackfish Creek (red triangles) are compared to an alluvial stream (black circles) in a mountain meadow (Arp unpublished data, stream described in Arp et al., 2007); all three streams had similar discharges ranging from 85 to 140 L s^{-1} during tracer tests and slopes ranging from 0.1 to 0.2 %, but with otherwise differing morphologies (experimental data and inverse modeling results shown in Table 3).

In beaded streams on the ACP, we have observed that peak flows predictably occur only 1–2 days after streams begin to flow initially, which is first on top of the ice and often partly beneath the rapidly melting snowpack in stream gulches. Over 5 a of gauging on five separate beaded streams, the timing of peak flows ranged from 1 to 10 June with peak hourly discharges of 1–10 m^3 s^{-1}, which typically exceeds summer flows by 2 orders of magnitude or more. This fast consistent response is similar to that observed for larger river systems of the ACP (Arp et al., 2012b; Bowling et al., 2003), which are fed predominantly by beaded streams and their source-water lakes. A related characteristic is that water temperatures are very near 0 °C at flow initiation and rise very rapidly directly following peak discharge, often warming to 10 °C or more over a 2–3 day period (Fig. 13). These rapid changes in flow and temperature regimes may provide important cues to fish migrating along larger river courses fed by beaded streams. Arctic graylings (*Thymallus arcticus*) are known to seek habitats that warm most rapidly in the spring to spawn, and the quickly rising temperatures of beaded streams may contribute to their importance as spawning habitats (Heim, 2014). In fact, we often see individual fish migrating up beaded channels with water flowing over bedfast ice just prior to peak flows, when their dark bodies can be easily observed crossing the white ice surface. Tracking studies of Arctic grayling tagged in Crea Creek, show a rapid pulse of upstream migration into the system during and after peak flow (Heim, 2014). This early upstream migration may represent an adaption to maximize time spent in produc-tive spawning habitats at the earliest possible time in order to provide a longer period of growth for offspring.

More broadly, the period of peak flow across this hydrologic landscape represents a period of high connectivity among aquatic habitats, where fish can disperse from relatively limited deepwater overwintering habitats and move into shallow, seasonally flowing habitats like beaded streams. Again, in late August through September, changes in flow and temperature may become important environmental cues that fish use to time migratory movements out of beaded streams (Heim, 2014). Migration out of Crea Creek in the fall was strongly correlated to decreases in stream temperature, as the channel connection to the Ublutuoch River became restricted due to ice formation. Low flows and colder temperatures increase the risks of utilizing Crea Creek (Arctic grayling were not found to overwinter within the drainage), yet persistence of fish within the drainage through September may be advantageous in terms of growth and acquisition of energy reserves prior to the onset of winter (Heim, 2014).

With respect to the basic physics of flow through stream systems characterized by multiple evenly spaced pools (storage zones), the attenuation of flows seems intuitive. This has implications for streamflow dynamics, movement and transformations of solutes (carbon, nutrients, and contaminants), the transport of particles including mineral and organic sediment, plankton (both semimobile and drift), and the movement of fish. Because most beaded streams are set within a permafrost framework without interactions with groundwater systems, the development of hyporheic flow through bed material or banks is unlikely. Storage processes have been investigated in Imnavait Creek and adjacent beaded streams around Toolik Lake in Alaska where the glaciated setting and corresponding porous substrates, and known spring systems, may allow hyporheic storage to play a significant role in beaded stream hydrology (Merck et al., 2012; Zarnetske et al., 2007). Still, we suggest that the characteristic large size and frequency of pools of beaded streams strongly dominates transient storage, even when groundwater systems are present and allowing for hyporheic exchange, which is probably rare in continuous permafrost zones of the ACP where surface-water interactions with groundwater are absent.

The distribution of water velocity at the reach scale in a beaded stream with large, deep and coalesced pools (Blackfish Creek) compared to a stream with shallower elliptical pools (Crea Creek) using tracer tests highlights how such morphology functions in water storage and residence time (Fig. 14). For example, the much more rapid velocities observed in an alluvial channel with otherwise similar discharge and slope underscores this impact on dense, evenly spaced pools on the hydrologic functioning of beaded channels. A similar range of reach-scale velocities are reported when comparing beaded channels to other channel types in Arctic drainage networks (Tarbeev and Surkov, 2013, Zarnetske et al., 2007).

Table 3. Results from reach-scale tracer injections for Crea (325 m, shallow elliptical beads) and Blackfish (232 m, deep coalesced beads) creeks during the summer of 2013 (RWT is rhodamine WT, Q is stream discharge, A is the advective cross-sectional area, U is advective zone velocity, D is the dispersion coefficient, A_S is the storage zone cross-sectional area, A_S/A is the relative storage zone area, α is the storage zone exchange coefficient, A_R and U_R are the cross-sectional area and velocity, respectively, of a single channel run). Comparisons of these results are made to two other RWT tracer studies of similar sized streams with beaded and other channel morphologies.

Site	Experiment data			Total channel hydraulics				Channel storage zone			Channel run (single)	
	Date	Solute added (RWT, g)	Q $(\mathrm{m^3\,s^{-1}})$	A $(\mathrm{m^2})$	U $(\mathrm{m\,s^{-1}})$	D $(\mathrm{m^2\,s^{-1}})$	A_S $(\mathrm{m^2})$	A_S/A	α $(\mathrm{s^{-1}})$	A_R $(\mathrm{m^2})$	U_R $(\mathrm{m\,s^{-1}})$
beaded streams in Fish Creek watershed in 2013 (this study)												
Crea	14-Jun	70.4	1.17	5.29	0.22	3.33	5.32	1.01	1.9E-03	2.48	0.54
Crea	5-Jul	49.9	0.13	1.89	0.04	0.88	2.71	1.43	5.9E-04	0.43	0.39
Crea	25-Aug	19.9	0.03	1.95	0.01	0.38	2.55	1.31	1.2E-03	0.10	0.33
Blackfish	13-Jun	92.4	1.73	9.81	0.18	1.90	9.08	0.93	3.2E-03	2.90	0.70
Blackfish	6-Jul	41.4	0.09	7.00	0.01	0.45	6.60	0.94	1.5E-03	0.52	0.33
Blackfish	24-Aug	19.1	0.03	–	–	–	–	–	–	0.36	0.15
multiple stream types near Toolik Lake in 2004 (Zarnetske et al., 2007)												
Lake inlet	17-Jun	–	0.26	–	0.16	1.48	–	–	2.0E-4	–	–
Lake outlet	18-Jun	–	0.09	–	0.07	1.71	–	–	5.0E-4	–	–
Beaded	25-Jun	–	0.05	–	0.02	1.75	–	–	3.0E-4	–	–
Beaded	21-Jun	–	0.44	–	0.09	1.94	–	–	6.0E-4	–	–
multiple stream types in a mountain meadow in 2004 (Arp unpublished data, streams described in Arp et al., 2007)												
Alluvial	11-Aug	–	0.14	–	0.22	–	–	0.69	1.6E-4	–	–
Lake outlet	10-Aug	–	0.17	–	0.06	–	–	0.23	6.7E-4	–	–

Residence times of water in these two beaded channels increase predictably with decreasing flows and relatively higher storage areas (Table 3). At the start of peak-flow recession, over 10 % of the water in both channels was still moving at velocities lower than 0.1 m s^{-1}. During summer flows, the fastest reach-scale velocities did not exceed 0.2 m s^{-1} in Crea Creak and 0.05 m s^{-1} in Blackfish Creek. Even though individual run velocities often exceed 0.5 m s^{-1} or greater, the water in the channel exchanges with storage zones (pools) sufficiently to slow the total movement of water by up to an order of magnitude or much more. Such slow transport rates of water in beaded stream systems may have important implications for maintaining in-stream flow during dry summers when evapotranspiration far exceeds rainfall on daily to weekly timescales. The major source of water to these channels are upstream lakes (Arp et al., 2012b; Bowling et al., 2003), and the evenly spaced storage-rich nature of these streams may function to maintain more constant flows and reduce evaporative losses during summer drought periods.

The summer of 2013 when these experiments were conducted was very wet and rainy compared to previous years when we have monitored discharge in these streams. Still, in 5 a of monitoring, starting in the summer of 2008, we have not yet observed interruptions in flow during summer drought periods in the five gauged streams. At least some alluvial streams in the Arctic foothills of Alaska have experienced prolonged periods of no flow over certain reaches during drought conditions when only minimal flow through interstitial gravels disrupt migration of the Arctic grayling (Betts and Kane, 2011). In some instances, individual Arctic graylings have been observed traveling over 160 km within a year visiting different key habitats within a "migratory circuit" (West et al., 1992). Thus, connectivity among spatially separated habitats is critical to this life history strategy, and beaded streams may function in maintaining hydrologic connectivity and fish passage between alluvial rivers, tundra lakes and ponds. Extreme drought conditions occurred on the ACP and foothills during the summer of 2007 and the hydrologic response has been well documented in rivers (Betts and Kane, 2011; Arp et al., 2012b), thermokarst lakes (Jones et al., 2009a), and upland tundra (Jones et al., 2009b) in this region. Whether beaded streams in this area maintained hydrologic connectivity between river and lake systems through this dry summer was undocumented and warrants reconstruction through hindcast modeling.

The other key function that the hydraulics of beaded streams provides is productive foraging habitat for Arctic fishes. This stems from the observation that larger foraging fishes (e.g., Arctic grayling) spend much of their time holding in channel runs downstream of pools, where they efficiently ambush drifting zooplankton, invertebrates, and ninespine stickleback (McFarland, 2012). The rapid shift in velocities from pools to runs may function as a key delivery system of forage that either resides primarily in beaded stream pools (i.e., ninespine stickleback and aquatic macroinvertebrates) or comes downstream as drift from lakes
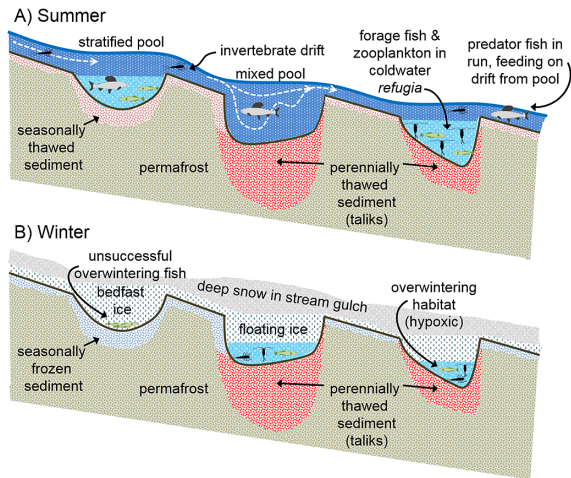
Figure 15. Conceptual diagram showing morphology, physical regimes, habitats, and organisms of a hypothetical pool-run system in the summer **(a)** and winter **(b)** based on observations and monitoring studies in multiple beaded stream systems during these time periods over many years.

(i.e., zooplankton) or laterally from riparian vegetation (i.e., terrestrial invertebrates). Such a setting may in part be the same reason why lake inlets and outlets are such productive ecosystems (Jones, 2010). The difference here is that along the course of beaded streams, this lake outlet delivery system is replicated multiple times over a short distance (i.e., 5 times per 100 m on average; Fig. 6). Approximately half of the Fish Creek drainage network is composed of beaded streams, the equivalent of 1200 km of stream length (Arp et al., 2012b). If we assume a pool density of five per 100 m, this gives us an estimated 60 000 pools (beads) throughout this watershed. Recently, the development of a Fish Creek watershed classification of lakes > 1 ha shows 4362 lakes, of which 45 % have perennial stream outlets and another 30 % have at least ephemeral outlets (B. M. Jones, unpublished data). In terms of potential fish habitat for summer foraging, this comparison suggests that pools in beaded streams increase the number of potential fish habitat zones for ambush foraging by 18-fold across the landscape over lake inlets and outlets alone.

4 Conclusions

This body of research on beaded streams in continuous permafrost landscapes documents a wide and varied distribution across the circum-Arctic in relation to ground-ice content in the upper permafrost, topography, and elevation. On the inner coastal plain of northern Alaska, our surveys indicate that beaded streams compose the majority of drainage networks and most channels initiate from and are fed by lakes. At least in northern Alaska, lakes supply water for new development in the form of ice roads and other industrial and municipal uses. Knowing how such practices af-

fect downstream ecosystems warrants investigation. Channels with beaded morphology are maintained downstream, eventually forming alluvial channels in relation to varied water and sediment supply. This suggests that new land disturbances, such as road construction or thermokarst processes that can alter these watershed fluxes, will factor into future drainage network changes. It also appears that beaded stream channels are relatively stable over time and potentially very old, such that any observations of rapid channel change may be indicative of more extreme forcing agents, either anthropogenic or climate driven. Given these concerns and the high density of beaded stream systems in many Arctic landscapes, expanded research into the role of these ecosystems in permafrost, hydrological, and biological processes will be essential.

The coupled biophysical processes of beaded stream systems that provide key ecosystem functionality are described conceptually in Fig. 15. We found high spatial and temporal thermal variability among pools, which likely play an important role in permafrost thaw and cold-water habitats (Fig. 15a). Beaded morphology appears to also play an important role in summer feeding habitats and hydrologic connectivity for migrating fish, the quality and availability of which is critical during short Arctic summers. During long Arctic winters, beaded stream gulches fill with deep snow that effectively insulates ice and permafrost and plays a role in creating taliks and providing overwintering habitats for certain fish and invertebrate communities (Fig. 15b). This conceptual understanding of beaded stream systems helps summarize seasonal and reach-scale ecosystem functions of interest to physical and biological scientists including managers concerned with changing human uses of Arctic lands and waters.

Edited by: J. Vonk

References

Armstrong, J. B., Schindler, D. E., Ruff, C. P., Brooks, G. T., Bentley, K. E., and Torgersen, C. E.: Diel horizontal migration in streams: Juvenile fish exploit spatial heterogeneity in thermal and trophic resources, Ecology, 94, 2066–2075, doi:10.1890/12-1200.1, 2013.

Arp, C. D., Schmidt, J. C., Baker, M. A., and Myers, A. K.: Stream geomorphology in a mountain lake district: hydraulic geometry, sediment sources and sinks, and downstream lake effects, Earth Surf. Proc. Land., 32, 525–543, doi:10.1002/Esp.1421, 2007.

Arp, C., Jones, B., Beck, R., Whitman, M., Derry, J., Lilly, M., and Grosse, G.: Variation in snow-water equivalent (SWE) among tundra, lakes, and streams on the Alaskan Arctic Coastal Plain: implications for regional SWE estimates and ice-thickness, Annual Conference of the American Water Resources Association, Phillidelphia, PA, November 2, 28, 2010.

Arp, C. D., Jones, B. M., Lu, Z., and Whitman, M. S.: Shifting balance of lake ice regimes on the Arctic Coastal Plain of northern Alaska, Geophys. Res. Lett., 39, 1–5, 2012a.

Arp, C. D., Whitman, M. S., Jones, B. M., Kemnitz, R., Grosse, G., and Urban, F. E.: Drainage network structure and hydrologic behavior of three lake-rich watersheds on the Arctic Coastal Plain, Alaska, Arct. Antarct. Alp. Res., 44, 385–398, 2012b.

Best, H., McNamara, J. P., and Liberty, L.: Association of ice and river channel morphology determined using ground-penetrating radar in the Kuparuk River, Alaska, Arct. Anarct. Alpi. Res., 37, 157–162, 2005.

Betts, E. and Kane, D. L.: Understanding the mechanisms by which a perennial Arctic stream appears intermittent, American Geophysical Union Fall Meeting, San Francisco, 2011.

Bowling, L. C., Kane, D. L., Gieck, R. E., Hinzman, L. D., and Lettenmaier, D. P.: The role of surface storage in a low-gradient Arctic watershed, Water Resour. Res., 39, 1087, doi:10.1029/2002WR001466, 2003.

Brewer, M. C.: The thermal regime of an arctic lake, Transactions of the American Geophysical Union, 39, 278–284, 1958.

Brosten, T. R., Bradford, J. H., McNamara, J. P., Zarnetske, J. P., Gooseff, M. N., and Bowden, W. B.: Profiles of temporal thaw depths beneath two arctic stream types using ground-penetrating radar, Permafrost Periglac., 17, 341–355, 2006.

Brown, J.: An estimation of ground ice, coastal plain, northern Alaska, US Army Cold Regions Research and Engineering Laboratory Hanover, NH, 22, 1968.

Brown, J., Ferrians, O. J., Heginbottom, J. A., and Melnikov, E. S.: Circum-arctic map of permafrost and ground ice conditions, National Snow and Ice Data Center, Boulder, CO, 1998.

Burn, C. R.: Tundra lakes and permafrost, Richards Island, western Arctic coast, Canada, Can. J. Earth Sci., 39, 1281–1298, doi:10.1139/E02-035, 2002.

Carter, L. D.: A Pleistocene sand sea on the Alaskan Arctic coastal plain, Science, 211, 381–383, 1981.

Carter, L. D. and Galloway, J. P.: Engineering Geologic Map of the Harrison Bay Quadrangle, Alaska, U.S. Geological Survey, Menlo Park, CA, 2005.

Craig, P. C. and McCart, P. J.: Classification of stream types in Beaufort Sea drainages between Prudhoe Bay, Alaska and the MacKenzie Delta, N.W.T., Canada, Arct. Alp. Res., 7, 183–198, 1975.

Crawford, R. H.: Structure of an air-breathing organ and the swim bladder in the Alaska blackfish, *Dallia pectoralis* Bean, Canadian Journal of Zoology, 52, 1221–1225, 1974.

Davis, N.: Permafrost: a guide to frozen ground in transition, University of Alaska Press, Fairbanks, 351 pp., 2001.

Ensom, T. P., Burn, C. R., and Kokelj, S. V.: Lake- and channel-bottom temperatures in the Mackenzie Delta, Northwest Territories, Can. J. Earth Sci., 49, 963–978, doi:10.1139/E2012-001, 2012.

Frohn, R. C., Hinkel, K. M., and Eisner, W. R.: Satellite remote sensing classification of thaw lakes and drained thaw lake basins on the North Slope of Alaska, Remote Sens. Environ., 97, 116–126, doi:10.1016/j.rse.2005.04.022, 2005.

Grosse, G., Jones, B., and Arp, C.: Thermokarst Lakes, Drainage, and Drained Basins, in: Treatise on Geomorphology, edited by: Schroder, J., Giardino, R., and Harbor, J., Academic Press, San Diego, 1–29, 2013.

Heim, K.: Seasonal Movements of Arctic Grayling in a Small Stream on the Arctic Coastal Plain, Alaska, M. S., School of Fisheries and Ocean Sciences, University of Alaska Fairbanks, Fairbanks, 82 pp., 2014.

Hinkel, K. M., Frohn, R. C., Nelson, F. E., Eisner, W. R., and Beck, R. A.: Morphometric and spatial analysis of thaw lakes and drained thaw lake basins in the western Arctic Coastal Plain, Alaska, Permafrost Periglac., 16, 327–341, 2005.

Jones, B. M., Arp, C. D., Hinkel, K. M., Beck, R. A., Schmutz, J. A., and Winston, B.: Arctic lake physical processes and regimes with implications for winter water availability and management in the National Petroleum Reserve Alaska, Environ. Manage., 43, 1071–1084, doi:10.1007/s00267-008-9241-0, 2009a.

Jones, B. M., Kolden, C. A., Jandt, R., Abatzoglou, J. T., Urban, F., and Arp, C. D.: Fire Behavior, Weather, and Burn Severity of the 2007 Anaktuvuk River Tundra Fire, North Slope, Alaska, Arct. Antarct. Alp. Res., 41, 309–316, doi:10.1657/1938-4246-41.3.309, 2009b.

Jones, B. M., Gusmeroli, A., Arp, C. D., Strozzi, T., Grosse, G., Gaglioti, B. V., and Whitman, M. S.: Classification of freshwater ice conditions on the Alaskan Arctic Coastal Plain using ground penetrating radar and TerraSAR-X satellite data, Int. J. Remote Sens., 34, 8267–8279, doi:10.1080/2150704x.2013.834392, 2013.

Jones, N. E.: Incorporating lakes within the river discontinuum: longitudinal changes in ecological characteristics in stream-lake networks, Can. J. Fish. Aquat. Sci., 67, 1350–1362, Doi 10.1139/F10-069, 2010.

Jorgenson, M. T. and Shur, Y.: Evolution of lakes and basins in northern Alaska and discussion of the thaw lake cycle, J. Geophys. Res., 112, 1–12, doi:10.1029/2006JF000531, 2007.

Jorgenson, M. T., Shur, Y. L., and Pullman, E. R.: Abrupt increase in permafrost degradation in Arctic Alaska, Geophys. Res. Lett., 33, 1–4, 2006.

Jorgenson, M. T., Romonovsky, V., Yoshikawa, K., Kanevskiy, M., Shur, Y., Marchenko, S., Brown, J., and Jones, B.: Permafrost characteristics of Alaska – a new permafrost map of Alaska, Ninth International Conference on Permafrost, Fairbanks, AK, 2008.

Kanevskiy, M., Shur, Y., Jorgenson, M. T., Ping, C-L., Michaelson, G. J., Fortier, D., Stephani, E., Dillon, M., and Tumskoy, V.:

Ground ice in the upper permafrost of the Beaufort Sea coast of Alaska, Cold Reg. Sci. Technol., 85, 56–70, 2013.

Lachenbruch, A. H.: Contraction theory of ice-wedge polygons: a qualitative discussion, Permaforst International Conference, Lafayette, Indiana, 63–70, 1966.

Lachenbruch, A. H., Brewer, M. C., Greene, G. W., and Marshall, B. V.: Temperatures in permafrost, in: Temperature, its Measurement and Control in Science and Industry, 791–803, 1962.

Manley, W. F. and Kaufman, D. S.: Alaska PaleoGlacier Atlas, Institute of Arctic and Alpine Research (INSTAAR), University of Colorado, Boulder, CO, 2002.

McFarland, J., Wipfli, M. W., and Whitman, M. S.: Feeding ecology of Arctic grayling in a small beaded stream on the Arctic Coastal Plain, Alaska, Conference of the Alaska Chapter of the American Fisheries Society, Kodiak, AK, 128, 23 October, 2012.

McKnight, D. M., Gooseff, M. N., Vincent, W. F., and Peterson, B. J.: High-latitude rivers and streams, in: Polar Rivers and Lakes, edited by: Vincent, W. F. and Laybourn-Parry, J., Oxford University Press, Oxford, 83–102, 2008.

McNamara, J. P., Kane, D. L., and Hinzman, L. D.: An analysis of an arctic channel network using a digital elevation model, Geomorphology, 29, 339–353, 1999.

Merck, M. F. and Neilson, B. T.: Modelling in-pool temperature variability in a beaded arctic stream, Hydrol. Process., 26, 3921–3933, doi:10.1002/Hyp.8419, 2012.

Merck, M. F., Neilson, B. T., Cory, R. M., and Kling, G. W.: Variability of in-stream and riparian storage in a beaded arctic stream, Hydrol. Process., 26, 2938–2950, doi:10.1002/Hyp.8323, 2012.

Montgomery, D. R. and Dietrich, W. E.: Source areas, drainage density, and channel initiation, Water Resour. Res., 25, 1907–1918, 1989.

Montgomery, D. R. and Buffington, J. M.: Channel-reach morphology in mountain drainage basins, Geol. Soc. Am. Bull., 109, 596–611, 1997.

Oswood, M. W., Everett, K. R., and Schell, D. M.: Some physical and chemical characteristics of an arctic beaded stream, Holarctic Ecol., 12, 290–295, 1989.

Pewé, T. L.: Ice-wedges in Alaska – classification, distribution, and climatic significance, Permafrost International Conference, Lafayette, Indiana, 1966, 76–81, 1966.

Reimer, P. J., Bard, E., Bayliss, A., Beck, J. W., Blackwell, P. G., Ramsey, C. B., Buck, C. E., Cheng, H., Edwards, R. L., Friedrich, M., Grootes, P. M., Guilderson, T. P., Haflidason, H., Hajdas, I., Hatte, C., Heaton, T. J., Hoffmann, D. L., Hogg, A. G., Hughen, K. A., Kaiser, K. F., Kromer, B., Manning, S. W., Niu, M., Reimer, R. W., Richards, D. A., Scott, E. M., Southon, J. R., Staff, R. A., Turney, C. S. M., and van der Plicht, J.: Intcal13 and Marine13 Radiocarbon Age Calibration Curves 0–50000 Years Cal Bp, Radiocarbon, 55, 1869–1887, 2013.

Rosgen, D. L.: A classification of natural rivers, Catena, 22, 169–199, 1994.

Runkel, R. L.: Using OTIS to model solute transport in streams and rivers, USGS, Denver, CO, Fact Sheet FS-138-99, 1–4, 2000.

Scott, K. M.: Effects of permafrost on stream channel behavior in Arctic Alaska, USGS, Washingtion, D. C., Geological Survey Professional Paper 1068, 1–19, 1978.

Scott, W. B. and Crossman, E. J.: Freshwater fishes of Canada, Fisheries Research Board of Canada, 966 pp., 1973.

Sturm, M., Racine, C., and Tape, K.: Increasing shrub abundance in the Arctic, Nature, 411, 546–547, 2001.

Tarbeeva, A. M. and Surkov, V. V.: Beaded channels of small rivers in permafrost zones, Geography and Natural Resources, 34, 27–32, doi:10.1134/S1875372813030049, 2013.

Vasudevan, D., Fimmen, R. L., and Francisco, A. B.: Tracer-grade rhodamine WT: structure of constituent isomers and their sorption behavior, Environ. Sci. Technol., 35, 4089–4096, 2001.

West, R. L., Smith, M. W., Barber, W. E., Reynolds, J. B., and Hop, H.: Autumn Migration and Overwintering of Arctic Grayling in Coastal Streams of the Arctic National Wildlife Refuge, Alaska, T. Am. Fish. Soc., 121, 709–715, doi:10.1577/1548-8659(1992)121<0709:Amaooa>2.3.Co;2, 1992.

Whiting, P. J. and Bradley, J. B.: A process-based classification system for headwater streams, Earth Processes and Landforms, 18, 603–612, 1993.

Whitman, M. S., Arp, C. D., Jones, B., Morris, W., Grosse, G., Urban, F., and Kemnitz, R.: Developing a long-term aquatic monitoring network in a complex watershed of the Alaskan Arctic Coastal Plain, in: Proceedings of the Fourth Interagency Conference on Research in Watersheds: Observing, Studying, and Managing for Change, 2011–5169 ed., edited by: Medley, C. N., Patterson, G., and Parker, M. J., Scientific Investigations Report, USGS, Reston, 15–20, 2011.

Wohl, E.: Mountain Rivers, Water Resources Monograph 14, American Geophysical Union, Washington, D.C., 320 pp., 2000.

Woo, M.: Permafrost Hydrology, Springer-Verlag, New York, 563 pp., 2012.

Zarnetske, J. P., Gooseff, M. N., Brosten, T. R., Bradford, J. H., McNamara, J. P., and Bowden, W. B.: Transient storage as a function of geomorphology, discharge, and permafrost active layer conditions in Arctic tundra streams, Water Resour. Res., 43, 1–13, doi:10.1029/2005WR004816, 2007.

Zarnetske, J. P., Gooseff, M. N., Bowden, W. B., Greenwald, M. J., Brosten, T. R., Bradford, J. H., and McNamara, J. P.: Influence of morphology and permafrost dynamics on hyporheic exchange in arctic headwater streams under warming climate conditions, Geophys. Res. Lett., 35, 1–5, doi:10.1029/2007GL032049, 2008.